

# *Ab initio* electronic structure calculation of hollandite vanadate $\text{K}_2\text{V}_8\text{O}_{16}$

M. Sakamaki<sup>1</sup>, S. Horiuchi<sup>2</sup>, T. Konishi<sup>1</sup>, and Y. Ohta<sup>2</sup>

<sup>1</sup>Graduate School of Advanced Integration Science, Chiba University, Chiba 263-8522, Japan and

<sup>2</sup>Department of Physics, Chiba University, Chiba 263-8522, Japan

(Dated: October 29, 2018)

An *ab initio* electronic structure calculation based on the generalized gradient approximation in the density functional theory is carried out to study the basic electronic states of hollandite vanadate  $\text{K}_2\text{V}_8\text{O}_{16}$ . We find that the states near the Fermi energy consist predominantly of the three  $t_{2g}$ -orbital components and the hybridization with oxygen  $2p$  orbitals is small. The  $d_{yz}$  and  $d_{zx}$  orbitals are exactly degenerate and are lifted from the  $d_{xy}$  orbital. The calculated band dispersion and Fermi surface indicate that the system is not purely one-dimensional but the coupling between the VO double chains is important. Comparison with available experimental data suggests the importance of electron correlations in this system.

PACS numbers: 71.30.+h, 71.20.Be, 71.28.+d

## I. INTRODUCTION

The metal-insulator phase transition associated with charge and orbital ordering has been one of the central issues in physics of strongly correlated electron systems. Recently, Isobe *et al.*<sup>1</sup> reported that the metal-insulator transition occurs in hollandite vanadate  $\text{K}_2\text{V}_8\text{O}_{16}$  at  $\sim 160$  K, which is accompanied by a rapid reduction of the magnetic susceptibility. A characteristic superlattice of  $\sqrt{2}a \times \sqrt{2}a \times 2c$  is observed below the transition temperature. A possible charge-ordering phase transition accompanied by the spin-singlet formation has thereby been suggested.<sup>1</sup> Quite recently, the phase diagram under high pressures has also been obtained,<sup>2</sup> where a variety of charge-ordered phases have been suggested to appear. The metal-insulator transition has also been observed in  $\text{Bi}_x\text{V}_8\text{O}_{16}$ <sup>3,4</sup> and  $\text{K}_2\text{Cr}_8\text{O}_{16}$ .<sup>5</sup>

The crystal structure of  $\text{K}_2\text{V}_8\text{O}_{16}$  belongs to a group of hollandite-type phases and has a  $\text{V}_8\text{O}_{16}$  framework composed of double strings of edge-shared  $\text{VO}_6$  octahedra. The system may be regarded as a one-dimensional version of  $\text{LiVO}_2$  known as a possible orbital-ordering system of the  $t_{2g}$  orbitals on the triangular lattice of  $S = 1$  spins.<sup>6</sup> The present system  $\text{K}_2\text{V}_8\text{O}_{16}$  has the average valence of  $\text{V}^{3.75+}$  and thus is in the mixed valent state of  $\text{V}^{3+} : \text{V}^{4+} = 3d^2 : 3d^1 = 1 : 3$ . Thus, the central issue in the present system is the mechanism of the metal-insulator transition concerning how the highly frustrated spin, charge, and orbital degrees of freedom at high temperatures are relaxed by lowering temperatures and what type of order is realized in the ground state.

In our previous paper,<sup>7</sup> we studied this material in the strong correlation limit; we set up a high-energy model Hamiltonian and applied a strong-coupling perturbation theory to obtain the low-energy effective spin-orbit Hamiltonian. The obtained effective Hamiltonian was analyzed numerically and the possible orbital and spin structure of the ground state of the system was proposed.<sup>7</sup>

However, so far not much is known even for the basic electronic states of the system, such as the band disper-

sion, Fermi surface, density of states, etc., both experimentally and theoretically. The purpose of the present paper is therefore to present an *ab initio* electronic structure calculation of this system to clarify its basic electronic structure. Here, we use the generalized gradient approximation (GGA) for the electron correlations in the density functional theory. The study is thus in the weak correlation limit but we hope that one can learn much of the basic electronic states of this material.

In this paper, we will show the following: The electronic states near the Fermi level are dominated by the three  $t_{2g}$ -orbital components, where the hybridization with the oxygen  $2p$  orbitals is small. The  $d_{yz}$  and  $d_{zx}$  orbitals are exactly degenerate and are lifted from the  $d_{xy}$  orbital (hereafter we use the notation of the axes  $x$ ,  $y$ , and  $z$  defined in Ref.,<sup>7</sup> also see Fig. 5 below). The calculated band structure and Fermi surface indicate that the system is not purely one-dimensional but the coupling between the VO double chains is important. We find no nesting features in the Fermi surfaces that contribute to the instability of the doubling of the unit cell along the  $c$  axis, suggesting the observed lattice instability to be the strong-coupling origin. We will compare our calculated results with experiment such as photoemission spectroscopy<sup>8</sup> and nuclear magnetic resonance (NMR),<sup>9</sup> from which we will discuss the implications on the electronic states and peculiarity of this material.

We hope that the present study, if combined with the strong-coupling approach, will give a reliable theory to explain the mechanism of the electronic phase transition of this intriguing material.

## II. METHOD OF CALCULATION

We here employ the computer code WIEN2k<sup>10</sup> based on the full-potential linearized augmented-plane-wave (FLAPW) method. We have tested both the local density approximation (LDA) and generalized gradient approximation (GGA) for the exchange-correlation potential<sup>11,12</sup> in the density functional theory. In this paper, we will

however present only the results of GGA because no significant differences are found between the results of LDA and GGA. The spin-orbit interaction is not taken into account. No spin-polarization is assumed. In the self-consistent calculations, we use 4,335  $\mathbf{k}$  points in the irreducible part of the Brillouin zone (see Fig. 1) with an anisotropic sampling in order to achieve better convergence. We use the plane-wave cutoff of  $K_{\max} = 4.24 \text{ Bohr}^{-1}$ .

We assume the experimental crystal structure of  $\text{K}_2\text{V}_8\text{O}_{16}$  observed at room temperature (above the metal-insulator transition) with the lattice constants of  $a = 9.963$  and  $c = 2.916 \text{ \AA}$ .<sup>13</sup> The Bravais lattice is body-centered tetragonal (see Fig. 1) and the primitive unit cell contains four V ions, one K ion, and eight O ions. We use the code XCrySDen<sup>14</sup> for graphical purposes.

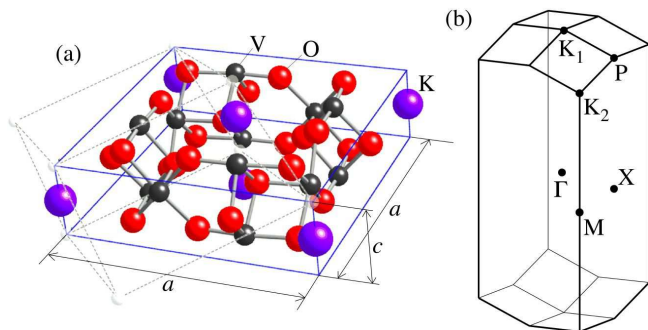


FIG. 1: (Color online) Schematic representation of (a) the unit cell of the body-centered tetragonal lattice (solid lines) and (b) Brillouin zone of  $\text{K}_2\text{V}_8\text{O}_{16}$ . In (a), the primitive unit cell is also shown in the thin dotted lines. In (b), the symbols represent  $\Gamma(0, 0, 0)$ ,  $M(2\pi/a, 0, 0)$ ,  $X(\pi/a, \pi/a, 0)$ ,  $P(\pi/a, \pi/a, \pi/c)$ ,  $K_1(0, 0, \pi(1/c + c/a^2))$ , and  $K_2(2\pi/a, 0, \pi(1/c - c/a^2))$ , where  $K_1$  and  $K_2$  are equivalent.

### III. RESULTS OF CALCULATION

#### A. Band dispersion

The calculated band dispersion near the Fermi energy is shown in Fig. 2. We find that there are 12  $t_{2g}$  bands of the V  $3d$  orbitals, 5 of which cross the Fermi level. We find the highly dispersive bands along the  $\Gamma$ - $K_1$ , X-P, and M- $K_2$  lines and weakly dispersive bands along the  $\Gamma$ -X, P- $K_1$ , and  $K_1$ - $K_2$  lines, reflecting the one-dimensionality of the electronic state. However, the band structure is not simple even near the Fermi energy, suggesting that the contributions from the three-dimensionality are not negligible; in particular, the relatively large dispersion along the  $\Gamma$ -M line reflects the coupling between the VO double chains. Thus, to consider the low-energy electronic properties of this system, the three-dimensionality or the coupling between the VO double chains is essential. This result is consistent with the observed rather

small anisotropy of the electric resistivity of the single crystal of this material.<sup>2</sup>

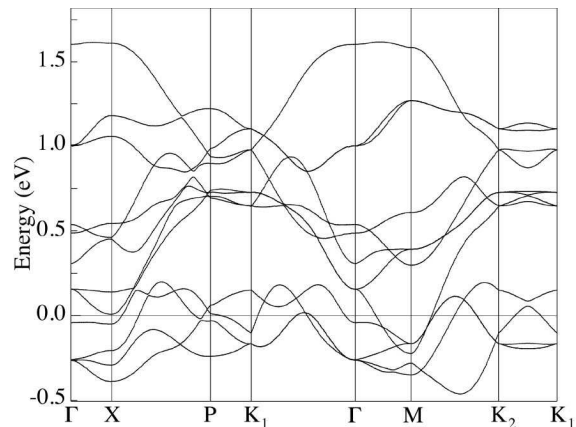


FIG. 2: Calculated band dispersion of  $\text{K}_2\text{V}_8\text{O}_{16}$  near the Fermi level (horizontal line). There are 12  $t_{2g}$  bands of the V  $3d$  orbitals, 5 of which cross the Fermi level. The labels of the  $\mathbf{k}$ -points are shown in Fig. 1.

#### B. Density of states

The calculated density of states is shown in Fig. 3, both in a wide energy range in (a) and near the Fermi energy in (b). We find that the V  $3d$  band is located between  $-0.5 \text{ eV}$  and  $4.5 \text{ eV}$  and is well separated from the O  $2p$  band located between  $-7.5 \text{ eV}$  and  $-2.5 \text{ eV}$ . The hybridization between V  $3d$  and O  $2p$  orbitals seems to be rather small, justifying the use of the strong-coupling model with only the  $d$  orbitals.<sup>7</sup> We also find that the  $t_{2g}$  band is well separated from the  $e_g$  band in the V  $3d$  bands, corresponding to a large value of the crystal field splitting of  $10D_q \simeq 2 \text{ eV}$ . Thus, the low-energy properties of this system is essentially governed by the three  $t_{2g}$  orbitals,  $d_{xy}$ ,  $d_{yz}$ , and  $d_{zx}$ .

The calculated orbital-decomposed partial densities of states  $\rho_\alpha(\varepsilon)$  ( $\alpha = xy, yz, zx$ ) are shown in Fig. 3(b). We first find that the total density of states at the Fermi level is very high, 30.4 states/f.u./eV (see Fig. 3(a)), which comes mainly from the three  $t_{2g}$  orbitals; the large ferromagnetic spin fluctuations observed in the NMR experiment<sup>9</sup> may be related to this high density of states at the Fermi level. We then find that the three  $t_{2g}$  orbitals equally contribute to the low-energy states near the Fermi energy. More precisely, we note that, even in the presence of the distortions of the  $\text{VO}_6$  octahedra, the relation  $\rho_{yz}(\varepsilon) = \rho_{zx}(\varepsilon)$  strictly holds. This is due to the inversion symmetry along the  $c$ -axis preserved even in the presence of the distortion.<sup>7</sup> We find that the width of the  $d_{xy}$  band is slightly smaller than the width of the  $d_{yz}$  and  $d_{zx}$  bands. We also find that the number of electrons in the  $d_{xy}$  orbital is slightly larger than that in the  $d_{yz}$  and  $d_{zx}$  orbitals; in the V atomic sphere, they are

0.345 and 0.246, respectively, in the energy range of the  $t_{2g}$  bands (see Sec. III D).

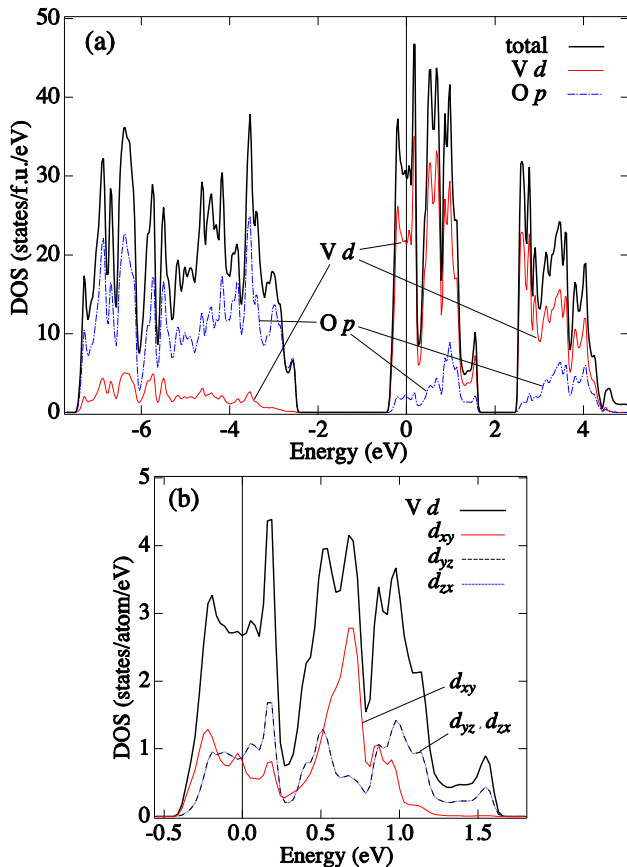


FIG. 3: (Color online) (a) Calculated density of states (per formula unit (f.u.)) of  $\text{K}_2\text{V}_8\text{O}_{16}$  in a wide energy range. (b) Calculated orbital-decomposed partial density of states (per atom) near the Fermi level. The Fermi level is indicated by the vertical line. Contributions from the  $d_{yz}$  and  $d_{zx}$  orbitals (thin dotted lines) are exactly degenerate.

### C. Fermi surface

The calculated results for the Fermi surface are shown in Fig. 4. There are 12  $t_{2g}$  bands, 5 of which cross the Fermi level and form the Fermi surface. If the system were strictly one-dimensional, a pair of the parallel Fermi surfaces should appear at  $k_z = \pm k_F$ . We actually find such types of the pairs of the Fermi surfaces in Figs. 4 (c) and (d), but the surfaces are rather distorted and moreover there are other types of the Fermi surfaces present. In particular, the Fermi surface shown in Fig. 4(e) comes from the dispersive band along the  $\Gamma$ -M line of the Brillouin zone (see Fig. 2) and is related to the coupling between the VO double chains. Therefore, we may conclude that the system is not purely one-dimensional, but the three-dimensionality or the coupling between the VO double chains is important.

We should point out that the possible nesting features in the two nearly-parallel Fermi surfaces seen in Fig. 4(c) does not lead to the  $2k_F$  instability corresponding to the observed<sup>1</sup> doubling of the unit cell along the  $c$  axis expected in the weak-coupling theory because the distance between the two Fermi surfaces is too short. No other Fermi surfaces are seen to contribute to the instability of the  $\sqrt{2}a \times \sqrt{2}a \times 2c$  superlattice formation. We therefore consider the observed lattice instability to be the strong-coupling origin, such as the long-range Coulomb interactions leading to charge orderings.<sup>7</sup>

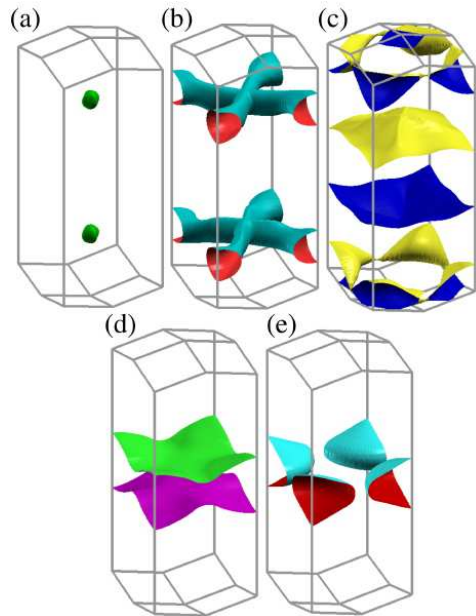


FIG. 4: (Color online) Calculated Fermi surfaces of  $\text{K}_2\text{V}_8\text{O}_{16}$ . The 53rd to 57th bands counted from the lowest are shown in (a) to (e), respectively.

### D. Valence electron distributions

The spatial distribution of the valence electrons of  $\text{K}_2\text{V}_8\text{O}_{16}$  in the energy range between  $-0.5$  eV and the Fermi level is shown in Fig. 5. The  $t_{2g}$  electrons mainly contribute to this distribution. We find that the result can be understood if we assume that the valence electrons are confined predominantly in the ligand field of each  $\text{VO}_6$  octahedron; i.e., the distribution can be projected mainly onto the  $d_{xy}$ ,  $d_{yz}$ , and  $d_{zx}$  orbitals. More precisely, however, we find that the distribution is somewhat compressed in the  $z$  direction (toward the apical O) and spread in the  $xy$  plane, indicating that the number of  $d_{xy}$  electrons is larger than that of  $d_{yz}$  and  $d_{zx}$  electrons. This is consistent with the results for the orbital-decomposed partial density of states (see Fig. 3), where the area below the Fermi level in the  $d_{xy}$  component is slightly larger than that in the  $d_{yz}$  and  $d_{zx}$  components.

We also note that the electron distribution reflects the symmetry that the  $d_{yz}$  and  $d_{zx}$  orbitals are equivalent. In the atomic limit, this degeneracy corresponds to the fact that the atomic energy levels of the  $d_{yz}$  and  $d_{zx}$  orbitals are exactly degenerate in the ionic model and are located slightly lower in energy than the atomic level of the  $d_{xy}$  orbital.<sup>7</sup> The orbital ordering in this system has thereby been suggested in the strong coupling theory.<sup>7</sup>

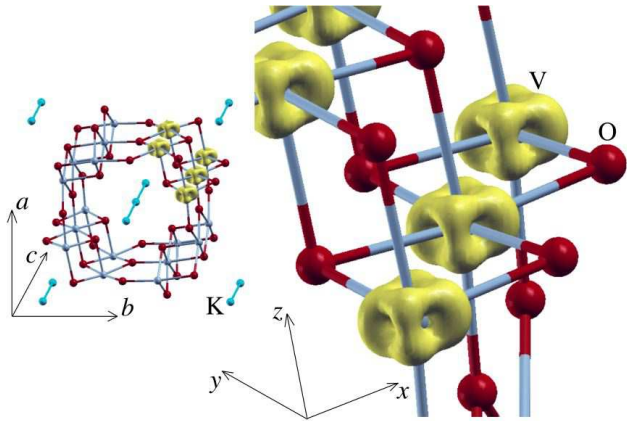


FIG. 5: (Color online) Calculated spatial density distributions of the valence electrons of  $\text{K}_2\text{V}_8\text{O}_{16}$  in the energy range between  $-0.5$  eV and the Fermi level, where the  $t_{2g}$  electrons mainly contribute. The isovalue of  $0.08$  electrons/Bohr<sup>3</sup> is used.

#### IV. DISCUSSION

Our calculated results presented here contains series of theoretical predictions, which should be checked by the experimental studies.

Let us first compare our calculated results with the results of the photoemission spectroscopy experiment.<sup>8</sup> It has been reported that, above the transition temperature, the coherent quasiparticle peak appears at the binding energy of  $\varepsilon_b \simeq 0 - 0.5$  eV (where the Fermi energy is set to 0), which we find corresponds well to the  $t_{2g}$  band below the Fermi energy shown in Fig. 3. The large incoherent spectral weight also appears at the binding energy of  $\varepsilon_b \simeq 0.5 - 2.5$  eV where a large gap with vanishing density of states appears in our calculated results (see Fig. 3). This result suggests the importance of electron correlations in this material; as has been pointed out in Ref.<sup>8</sup>, the situation is similar to the case of  $\text{V}_2\text{O}_3$ , for which the single-particle excitation spectra have been studied in detail.<sup>15</sup> The large and broad spectral weight appears at  $\varepsilon_b \simeq 2.5 - 9$  eV, which comes mainly from the O  $2p$  orbitals. The position and shape of this spectral weight agree well with our calculated density of states shown in Fig. 3.

Below the transition temperature, the coherent peak near the Fermi energy has been reported to shift largely

to higher binding energies, reflecting the opening of the quasiparticle gap of 230 meV.<sup>8</sup> The reconstruction of the electronic states by the metal-insulator transition should be pursued theoretically. However, the LDA and GGA calculations cannot reproduce the charge-ordered states with the spin-singlet formation. One needs to invent the strongly-correlated electron models to account for the phase transition, of which the simplest one-dimensional version has been proposed in Ref.<sup>7</sup>. Further study is required to take into account of the three-dimensionality of the system.

It has been reported in a recent NMR experiment<sup>9</sup> that there appears an exceptionally strong temperature dependence of the rotation of the NMR Knight-shift tensor, which suggests the strong orbital dependence of the local spin susceptibility. The degeneracy of the  $d_{yz}$  and  $d_{zx}$  orbitals may play a role here. We point out that the essential information should be obtained if the calculation of the spin density distribution under a uniform magnetic field can be made, which we leave for our future study.

It has also been reported<sup>2</sup> that, under high pressures, a variety of charge-ordered phases appear in this system; in particular, a different charge-ordered pattern with the antiferromagnetic long-range order has been suggested to occur above  $\sim 1$  GPa at low temperatures. Competing phases with similar energies have therefore been suggested to exist in this system, which should further be clarified both experimentally and theoretically.

#### V. SUMMARY

We have carried out the *ab initio* electronic structure calculation of hollandite vanadate  $\text{K}_2\text{V}_8\text{O}_{16}$  to clarify its basic electronic states in the weak correlation limit. We have shown the following:

- (i) The states near the Fermi level consist predominantly of the three  $t_{2g}$  orbitals and the hybridization with the oxygen  $2p$  orbitals is small. The strong-coupling model based on the three  $t_{2g}$  orbitals may therefore be justified.
- (ii) The  $d_{yz}$  and  $d_{zx}$  orbitals are exactly degenerate and are lifted from the  $d_{xy}$  orbital. The doubly-degenerate atomic energy levels may play a role in the observed electronic properties of the system.
- (iii) The calculated band structure and Fermi surface indicate that the system is not purely one-dimensional but the coupling between the VO double chains is important.
- (iv) No nesting features in the Fermi surfaces that contribute to the instability of the doubling of the unit cell along the  $c$  axis are seen, suggesting the observed lattice instability to be the strong-coupling origin.
- (v) The presence of strong electron correlations is suggested in the observed valence-band photoemission spectra compared with the calculated density of states.

We hope that the present results obtained in the weak correlation limit will be combined with the theory based on the strongly-correlated electron models in near future,

to help us understand the nature of the charge, orbital, and spin degrees of freedom of this intriguing material.

### Acknowledgments

We would like to thank M. Isobe, M. Itoh, Y. Shimizu, A. Yamasaki, and T. Yamauchi for useful dis-

cussions on the experimental aspects of  $K_2V_8O_{16}$ . This work was supported in part by Grants-in-Aid for Scientific Research (Nos. 18028008, 18043006, 18540338, and 19014004) from the Ministry of Education, Culture, Sports, Science and Technology of Japan. A part of computations was carried out at the Research Center for Computational Science, Okazaki Research Facilities, and the Institute for Solid State Physics, University of Tokyo.

- 
- <sup>1</sup> M. Isobe, S. Koishi, N. Kouno, J. Yamaura, T. Yamauchi, H. Ueda, H. Gotou, T. Yagi, and Y. Ueda, *J. Phys. Soc. Jpn.* **75**, 73801 (2006).
- <sup>2</sup> T. Yamauchi, H. Ueda, M. Isobe, and Y. Ueda, unpublished (2008).
- <sup>3</sup> T. Waki, H. Kato, M. Kato, and K. Yoshimura, *J. Phys. Soc. Jpn.* **73**, 275 (2004).
- <sup>4</sup> Y. Shibata and Y. Ohta, *J. Phys. Soc. Jpn.* **71**, 513 (2002).
- <sup>5</sup> K. Hasegawa, M. Isobe, T. Yamauchi, H. Ueda, J. Yamaura, H. Goto, T. Yagi, H. Sato, and Y. Ueda, unpublished.
- <sup>6</sup> H. F. Pen, J. van den Brink, D. I. Khomskii, and G. A. Sawatzky, *Phys. Rev. Lett.* **78**, 1323 (1997).
- <sup>7</sup> S. Horiuchi, T. Shirakawa, and Y. Ohta, *Phys. Rev. B* **77**, 155120 (2008).
- <sup>8</sup> A. Higashiya, A. Yamasaki, H. Fujiwara, J. Yamaguchi, A. Sekiyama, S. Imada, M. Isobe, Y. Ueda, T. Ishikawa, and S. Suga, unpublished.
- <sup>9</sup> Y. Shimizu, K. Okai, M. Itoh, M. Isobe, J. Yamaura, and Y. Ueda, unpublished.
- <sup>10</sup> P. Blaha, K. Schwarz, G. K. H. Madsen, D. Kvasnicka, and J. Luitz, *WIEN2k, An Augmented Plane Wave + Local Orbitals Program for Calculating Crystal Properties* (Technische Universität Wien, Austria, 2002); <http://www.wien2k.at>.
- <sup>11</sup> J. P. Perdew and Y. Wang, *Phys. Rev. B* **45**, 13244 (1992).
- <sup>12</sup> J. P. Perdew, K. Burke, and M. Ernzerhof, *Phys. Rev. Lett.* **77**, 3865 (1996).
- <sup>13</sup> W. Abriel, F. Rau, and K. J. Range, *Mater. Res. Bull.* **14**, 1463 (1979).
- <sup>14</sup> A. Kokalj, *Comp. Mater. Sci.* **28**, 155 (2003).
- <sup>15</sup> S.-K. Mo, J. D. Denlinger, H.-D. Kim, J.-H. Park, J. W. Allen, A. Sekiyama, A. Yamasaki, K. Kadono, S. Suga, Y. Saitoh, T. Muro, P. Metcalf, G. Keller, K. Held, V. Eyert, V. I. Anisimov, and D. Vollhardt, *Phys. Rev. Lett.* **90**, 186403 (2003).